



NRC Publications Archive Archives des publications du CNRC

Effects of particle size distribution and oxygen concentration on the propagation behavior of pulverized coal flames in O₂/CO₂ atmospheres

Gu, Mingyan; Chen, Xue; Wu, Cengceng; He, Xianhui; Chu, Huaqiang; Liu, Fengshan

This publication could be one of several versions: author's original, accepted manuscript or the publisher's version. / La version de cette publication peut être l'une des suivantes : la version prépublication de l'auteur, la version acceptée du manuscrit ou la version de l'éditeur.

For the publisher's version, please access the DOI link below. / Pour consulter la version de l'éditeur, utilisez le lien DOI ci-dessous.

Publisher's version / Version de l'éditeur:

<https://doi.org/10.1021/acs.energyfuels.6b03248>

Energy & Fuels, 31, 5, pp. 5571-5580, 2017-03-30

NRC Publications Record / Notice d'Archives des publications de CNRC:

<https://nrc-publications.canada.ca/eng/view/object/?id=745ac6c4-70a1-4989-b14f-b250b78eb584>

<https://publications-cnrc.canada.ca/fra/voir/objet/?id=745ac6c4-70a1-4989-b14f-b250b78eb584>

Access and use of this website and the material on it are subject to the Terms and Conditions set forth at

<https://nrc-publications.canada.ca/eng/copyright>

READ THESE TERMS AND CONDITIONS CAREFULLY BEFORE USING THIS WEBSITE.

L'accès à ce site Web et l'utilisation de son contenu sont assujettis aux conditions présentées dans le site

<https://publications-cnrc.canada.ca/fra/droits>

LISEZ CES CONDITIONS ATTENTIVEMENT AVANT D'UTILISER CE SITE WEB.

Questions? Contact the NRC Publications Archive team at

PublicationsArchive-ArchivesPublications@nrc-cnrc.gc.ca. If you wish to email the authors directly, please see the first page of the publication for their contact information.

Vous avez des questions? Nous pouvons vous aider. Pour communiquer directement avec un auteur, consultez la première page de la revue dans laquelle son article a été publié afin de trouver ses coordonnées. Si vous n'arrivez pas à les repérer, communiquez avec nous à PublicationsArchive-ArchivesPublications@nrc-cnrc.gc.ca.



National Research
Council Canada

Conseil national de
recherches Canada

Canada

Effects of Particle Size Distribution and Oxygen Concentration on the Propagation Behavior of Pulverized Coal Flames in O₂/CO₂ Atmospheres

Mingyan Gu,^{*,†} Xue Chen,[†] Cengceng Wu,[†] Xianhui He,[†] Huaqiang Chu,^{*,†,‡} and Fengshan Liu[‡]

[†]School of Energy and Environment, Anhui University of Technology, Ma'anshan 243000, China

[‡]Measurement Science and Standards, National Research Council, Ottawa, Ontario, Canada K1A 0R6

ABSTRACT: The ignition and flame propagation behavior of pulverized coal particles in an O₂/CO₂ atmosphere was studied in a long quartz tube reactor. The effects of mixing ratio of fine (mean diameter 16 μm) and coarse (mean diameter 82 μm) coal particles and oxygen concentration on the ignition characteristics, flame front distance, and flame propagation velocity were investigated by capturing the flame ignition and propagation using a high-speed video camera. The experimental results show that the particle size distribution has a strong influence on the ignition and flame structure of coal particles. Smaller coal particles result in earlier ignition, a smoother flame front, longer flame, and faster flame propagation velocity. Mixing of smaller coal particles with larger ones shortens the ignition delay and enhances the propagation velocity of the flame front. For different coal particle size distributions, the variation of flame propagation velocity with time in general displays an “M”-shaped curve. The curve of flame propagation velocity vs time is single-peaked at 40% oxygen concentration for both coarse and fine particles with mean diameters of 82 and 16 μm, respectively. The effect of oxygen concentration on the flame propagation becomes stronger as the percentage of fine particles increases. The effect of fine coal particles on the volatile release rate of coarse particles was analyzed by numerical simulation. The results show that increasing the ratio of fine coal particles shortens the time for volatile matter release from the coarse coal particles and increases the coarse particle temperature.

1. INTRODUCTION

The combustion technology of burning coal in O₂/CO₂ atmosphere has drawn widespread attention since it produces high-concentration CO₂ in the product, which is suitable for CO₂ capture and sequestration, and lowers pollutant emissions at the same time.^{1,2} The ignition delay and flame propagation velocity are important properties to assess the combustion efficiency and safety of pulverized coal and have been studied in different ways.^{3,4} The combustion characteristics of coal particles in the O₂/CO₂ atmosphere differ significantly from those in air.^{5,6} For example, a high CO₂ concentration increases the specific heat and the radiative transfer ability of the gas mixture and enhances the chemically prohibitive role of CO₂ in chemical reactions, which in turn leads to longer ignition delay, lower flame temperature, weakened flame stability, and reduced overall burning rate.^{7,8}

Jones et al. investigated the flame temperatures of coal particles in O₂/CO₂ atmosphere under different exhaust gas recirculation (EGR) ratios using charge-coupled device (CCD). It was found that the flame temperature decreases with increasing CO₂ concentration.⁹ Suda et al.¹⁰ conducted an experimental study of the flame propagation speed of coal particles under microgravity. Their results showed that the flame propagation velocity in an O₂/CO₂ atmosphere is only about 1/3 to 1/5 of that in air. To overcome the difficulties of coal combustion in O₂/CO₂ atmospheres of low O₂ and high CO₂ concentrations, it has been suggested to increase the oxygen concentration. Liu et al. studied the ignition characteristics of coal particles by utilizing a diffusion-flame-based Hencken burner.¹¹ They found that increasing the oxygen concentration is efficient in reducing the ignition delay.

Unfortunately, a higher oxygen concentration also enhances NO_x formation.¹² Therefore, increasing O₂ concentration in an O₂/CO₂ atmosphere for the purposes of improving the ignition and stability of coal combustion is clearly not a good option from the perspective of reducing pollutant emissions. A novel and potentially effective approach to improve the ignition and stability of coal flames without the penalty of increasing NO_x formation is to manipulate the fuel (pulverized coal) characteristics.

It has been known that the ignition and combustion characteristics of coal particles are strongly influenced by their sizes.^{13,14} For smaller coal particles, especially for superfine ones with particle diameter $d_p < 20$ μm, the particle temperature rise is faster and the ignition delay time is shorter.^{15–17} Compared to coarse coal particles, fine coal particles have the advantages of high burning rate, high combustion efficiency, and low NO_x formation. However, fine coal particles are more energy consumption to produce and their storage is also a concern.

In this study, the ignition and combustion behavior of different proportions of pulverized coal consisting of fine particles (mean diameter 16 μm) and coarse particles (mean diameter 82 μm) were conducted at different concentrations of O₂/CO₂ atmospheres to study the effects of particle size and oxygen concentration. The ignition and flame propagation of coal particles in a long quartz tube were recorded by a high-speed video camera. The objective is to gain insights into how

Received: December 23, 2016

Revised: March 30, 2017

Published: March 30, 2017

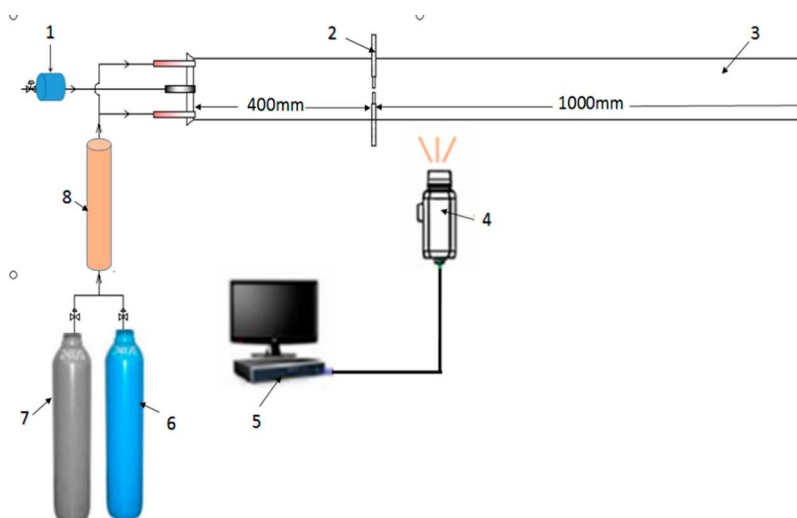


Figure 1. Schematic diagram of pulverized coal flame propagation measurement system.

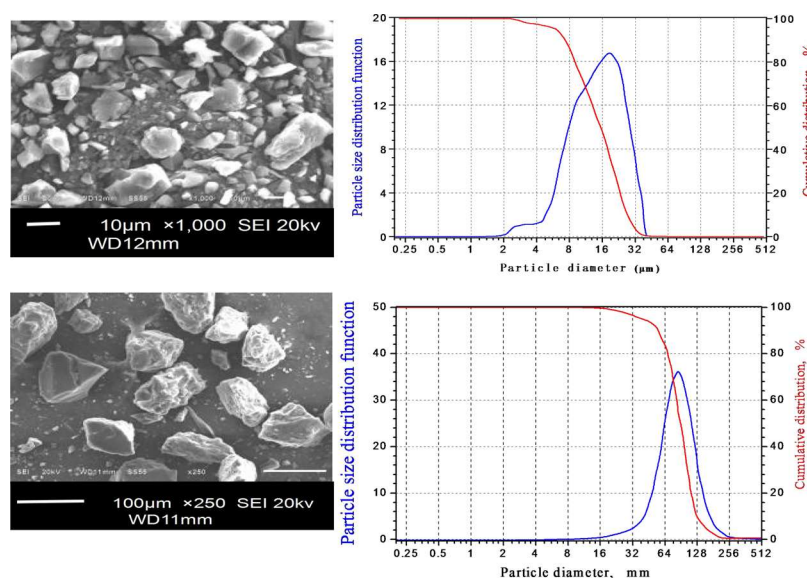


Figure 2. SEM images (left column) and the measured particle size distributions (right column) of the fine (top row) and coarse (bottom row) coal particles.

the mixing proportion of the fine coal particles into the coarse ones, while keeping the total particle mass flow rate constant, and the oxygen concentration influence the ignition and flame propagation in O_2/CO_2 atmosphere. The results of this study are believed to be highly valuable to assess the potential of using blended coal particles containing a mixture of fine and coarse coal particles as a novel method to simultaneously improve the ignition performance and reduce pollutant emissions of coal combustion in O_2/CO_2 atmospheres.

2. EXPERIMENTAL SETUP

A schematic of the experimental setup is shown in Figure 1. The inner diameter and length of the quartz glass tube are 7 and 140 cm, respectively. The right end of the tube is open, the oxidizer gas mixture inside the tube was supplied from the left side (enclosed with a rubber stopper), and the desired compositions were controlled by valves positioned on the top of the cylinders of O_2 and CO_2 gases. The coal particles (0.4 g in the present study) were injected through a nozzle installed in the center of the left end of the quartz tube, Figure 1. The nozzle was connected to a cylinder tank of 2.6 cm inner diameter and

10 cm in length (1 in Figure 1) with a copper pipe with an inner diameter of 8 mm. The cylinder tank was equipped with a piston-actuated valve capable of producing an instantaneous pressure of 0.6 MPa once the valve was actuated. Before each experiment, the valve in the cylinder tank (1 in Figure 1) was pulled to the far left position and locked by a mechanical switch. The entire system (the cylinder tank and the quartz tube) was then charged with the oxidizer gas mixture until a stable gas composition profile inside the quartz tube was established and the O_2 concentration at the outlet of the tube was monitored until it reached the designed level. When the oxygen concentration in the O_2/CO_2 atmosphere inside the tube reached the prescribed level, the valve inside the cylinder tank was actuated to produce a rapid compression between the valve and the injection nozzle and the coal particles were injected into the quartz tube through a 2 mm diameter hole. Under the action of the high-speed carrier oxidizer gas, a pulverized coal jet was formed inside the quartz tube with intense mixing between the coal jet and the oxidizer gas. Based on the high-speed video images, it took about 60 ms for the injected coal particles to reach to ignition electrodes (2 in Figure 1). The coal particle stream was ignited by an electric spark at a distance of 40 cm from the left end of tube (2 in Figure 1). The ignition power was 40 W, and the separation gap between the electrodes was 1.4 cm.

The flame propagation process was recorded by a high-speed video camera (Phantom V311).

A Chinese coal provided by China Shenhua was used in the present experimental study. After grinding and sieving, two different groups of coal particles were acquired: fine particles less than 20 μm in diameter and coarse particles having diameters between 70 and 100 μm . The coal particle size distribution was determined by a laser particle size analyzer (OMEC LS-C(IIA)). Figure 2 shows the SEM (scanning electron microscope) images and the measured particle size distributions of the fine and coarse coal particles. The mean diameters of the fine and coarse particles are 16 and 82 μm . Hereafter, the fine and coarse coal particles are named as D_{16} and D_{82} , respectively. Experiments were conducted for five coal particle samples, which were prepared by mixing D_{82} and D_{16} coal particles according to the following five mass ratios of 1:0, 7:3, 5:5, 3:7, and 0:1. The total mass of each coal samples was kept constant. All the five coal particle samples were baked in an oven set to 105 $^{\circ}\text{C}$ for 24 h before being used in the experiment. The proximate analysis of the Shenhua coal is provided in Table 1. The atmosphere (oxidizer) in which the

Table 1. Properties of Coal (dry, %)

proximate analysis of coal			ultimate analysis of coal				
ash	V	FC	C	H	O	N	S
4.91	29.45	65.64	75.26	4.51	19.21	0.86	0.16

combustion of coal particles takes place considered in the experiments is either air or an O_2/CO_2 mixture. The initial gas and coal particle temperatures are 298 K. Experiments were carried out for three oxygen concentrations (volumetric basis) of 30, 35, and 40% in the O_2/CO_2 atmosphere, as summarized in Table 2.

Table 2. Experimental Parameters

gas composition	mass ratio of coarse-to-fine particles
$V_{\text{O}_2} = 30\%$	$D_{82}:D_{16} = 1:0, 7:3, 5:5, 3:7, 0:1$
$V_{\text{O}_2} = 35\%$	$D_{82}:D_{16} = 1:0, 7:3, 5:5, 3:7, 0:1$
$V_{\text{O}_2} = 40\%$	$D_{82}:D_{16} = 1:0, 7:3, 5:5, 3:7, 0:1$
air	$D_{82}:D_{16} = 1:0, 7:3, 5:5, 3:7, 0:1$

3. NUMERICAL MODEL

To help understand the effects of mixing fine coal particles to coarse ones on volatile release, particle temperature rise, and ignition, a simplified numerical model was proposed. To highlight the role played by fine coal particles, the following assumptions are made in our simplified analysis of heat transfer, volatile release, and ignition of coal particles comprising of two monotonic sizes of 16 and 82 μm :

- (1) The fine and coarse coal particles are evenly distributed in a control volume of unit volume. The numbers of fine and coarse coal particles in the cell are specified according to their mass ratio. While the mass ratio of coarse-to-fine coal particles is varied, the total mass of fine and coarse coal particles is kept constant.
- (2) The coal particles are stationary in the control volume filled with air or an O_2/CO_2 mixture. The stoichiometric conditions are maintained under all the computational conditions considered. The total pressure of the control volume is kept at 1 atm. A change in the O_2 concentration is realized by adjusting the partial pressures of O_2 and CO_2 .
- (3) The control volume containing the coal particles and O_2/CO_2 mixture is adiabatic, i.e., it has no heat exchange

with the outside. The burning rate of the released volatile matters is assumed infinitely fast.

Under these assumptions, the particle mass conservation can be expressed as

$$\frac{dm_p}{d\tau} = \dot{m}_v + \dot{m}_c \quad (1)$$

which indicates that the particle mass change is caused by volatile release and char burnout, where m_p is the coal mass, \dot{m}_v is the devolatilization rate, and \dot{m}_c is the char burning rate. Various devolatilization models have been developed to describe the rate of compositions of volatile release process and some differences among the results of these models exist both in air and O_2/CO_2 atmosphere.^{7,18} In this study, the devolatilization process was modeled using the two-competition model.¹⁹ The devolatilization process is described by two competing overall reactions, and its rate is given as

$$\dot{m}_v = -m_p(R_1 + R_2)(\alpha_1 R_1 + \alpha_2 R_2) \quad (2)$$

where α_1 and α_2 are weights of each rate, and R_1 and R_2 are the two competing kinetic rates expressed in the Arrhenius form as

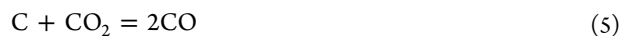
$$R_i = A_i \exp(-E_i/RT_p), \quad i = 1, 2 \quad (3)$$

The pre-exponential constant A_i and the activation energy E_i are listed in Table 3. Symbol T_p stands for the particle temperature.

Table 3. Kinetic Constants

reaction	A (units)	E (J/kg·mol)
R_1	3.7×10^5 ¹⁹ (s^{-1})	7.366×10^7 ¹⁹
R_2	1.46×10^{13} ¹⁹ (s^{-1})	2.511×10^8 ¹⁹
$\text{C} + \text{O}_2 \rightarrow \text{CO}_2$	1.255×10^3 ²¹ (m/s)	9.977×10^7 ²¹
$\text{C} + \text{CO}_2 \rightarrow 2\text{CO}$	4.016×10^8 ²¹ (m/s)	1.255×10^8 ²¹

The kinetic/diffusion surface reaction model is used to describe the char burnout process. The char burnout is assumed to take place through the following reactions



The char reaction rate is calculated as

$$\dot{m}_c = -A_p \rho_g RT_g \sum \left(\frac{Y_j}{M_{w,j}} \frac{1}{k_{s,j} + \frac{1}{k_{d,j}}} \right), \quad j = \text{O}_2, \text{CO}_2 \quad (6)$$

where A_p , T_g , and ρ_g are the particle surface area, gas temperature, and gas density, respectively. Y_j is the mass fraction of j gas, $M_{w,j}$ is molecular weight of j gas, and the kinetic rate $k_{s,j}$ is expressed in the Arrhenius form as

$$k_{s,j} = A_j \exp(-E_j/RT_p) \quad (7)$$

and the corresponding rate constants are also given in Table 3. The diffusion rate $k_{d,j}$ is written as²⁰

$$k_{d,j} = C_{\text{diff},j} \frac{((T_p + T_g)/2)^{0.75}}{d_p} \quad (8)$$

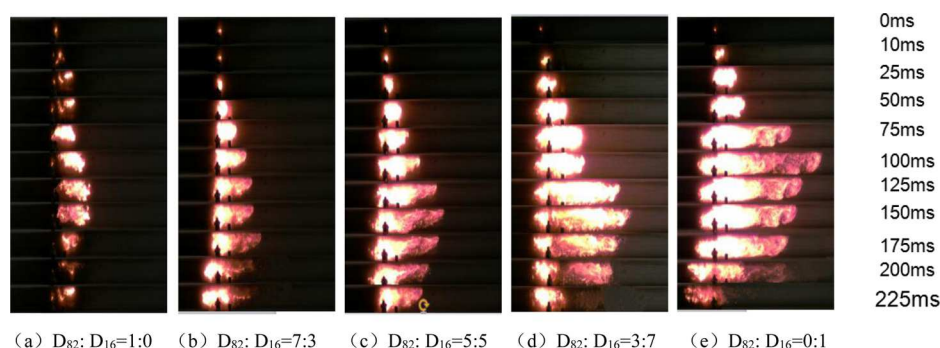


Figure 3. Evolution of coal ignition and flame propagation in the five coal samples ($V_{O_2} = 35\%$, O_2/CO_2 atmosphere).

where C_{diff} is equal to 4.0×10^{-12} for reaction 4 and 1.8×10^{-12} for reaction 5²⁰ in O_2/CO_2 atmospheres.

The coal particle temperature variation is governed by the following unsteady energy conservation equation

$$m_p c_p \frac{dT_p}{dt} = \dot{m}_v \Delta h_v + \dot{m}_c \Delta h_c + \frac{2\lambda}{d_p} A_p (T_g - T_p) \quad (9)$$

where c_p is the coal particle specific heat, Δh_v and Δh_c are the heat of volatile reaction and char reaction, respectively, and λ is the gas thermal conductivity. The last term on the right-hand side of eq 9 stands for the heat conduction rate between the coal particle and the surrounding gas.

4. EXPERIMENTAL RESULTS AND ANALYSIS

4.1. Coal Ignition and Flame Propagation Characteristics. Figure 3 displays the entire process of coal ignition and subsequent flame propagation as captured by the high-speed video camera for the five coal particle samples. For each coal sample, the combustion process can be characterized by the following three stages: the ignition stage, where the rate of coal devolatilization and burning intensity are low; the rapid burning stage in which a large amount of volatile matter is released and burning with a rapid movement of flame front; followed by the postflame stage, where separate/isolated burning char particles appear and the flame front retreats due to burnout of volatile and char particles.

As shown in Figure 3, the flame front movement was strongly affected by the coal particle size distribution, which is altered by the mass ratio of the coarse-to-fine coal particles in this study. It is evident from Figures 3a and e that the coal particle flame front of D_{82} (coarse coal particles) moves much slower than that of D_{16} (fine coal particles).

The D_{82} coal particles take a fairly long time (about 50–75 ms) after ignition to evolve from a tiny burning spot into a somewhat weak coal flame about 50 to 100 mm in length formed by few isolating burning spots. On the other hand, the D_{16} coal particles start to form a bright burning spot about 20 mm in size at 5 ms after ignition. The flame envelop of D_{16} coal particles also appears much smoother and grows much faster in size. Moreover, they differ in how the flame propagates. The D_{82} coal flame propagates slowly and the flame grows only up to about 200 mm in the entire combustion process, Figure 3a. After the maximum flame length is reached, the flame brightness fades quickly. In contrast, the D_{16} coal flame expands quickly into a bright flame-ball like structure between 0 and 25 ms, Figure 3e, and then propagates rapidly to fill nearly the entire quartz tube at 100 ms, the flame remains quite bright for a much longer period of time. The different behaviors of D_{82}

and D_{16} coal flames can be explained using the well-established coal combustion theory. For larger sized coal particles D_{82} , their temperature rise is much slower and hence they reach significantly lower temperatures than those of smaller particles (D_{16}) under the same ignition condition. Consequently, the devolatilization rate of larger coal particles is much lower and so are the initial development of the flame associated with the gas-phase reactions and the overall burning intensity. With a moderate amount of D_{16} mixing into the coal sample, Figure 3b, the flame kernel grows faster than the D_{82} coal flame, Figure 3a, and appears as fairly bright at 25 ms after ignition with 20 mm flame size. Subsequently, the flame expands and propagates to form a longer flame. It is clear from the flame photos shown in Figure 3 that with increasing proportion of D_{16} in the coal sample the initial ignition kernel requires a shorter time to evolve into a bright flame, suggesting a shorter ignition delay, and the flame propagates faster to reach a longer length. The results shown in Figure 3 indicate that mixing fine coal particles into coarse ones benefits significantly the ignition and subsequent propagation of a coal flame.

After the flame front reaches its maximum value in the quartz tube, the burning region starts to shrink and the flame brightness gradually fades away. A closer examination of the flame photos reveals that there are isolated burning particles, suggesting that char combustion is taking place at this stage. The fading flame brightness of the flame front at this stage is attributed to the burnout of volatile and the decreasing char combustion intensity. Although char combustion likely occurs around the moment of the maximum flame front position, especially for fine coal particles, its intensity decreases quickly in the absence of volatile combustion and excessive heat loss from char to the surroundings through convection, conduction, and radiation.

It can be observed from Figure 3 that the flame front gradually develops an asymmetric shape with respect to the quartz tube centerline, especially at longer times or at a larger proportion of fine coal particles in the coal samples. For example, at 75 ms in Figure 3e the upper part of the flame front reaches a larger distance than the lower part and this feature remains until the flame front luminosity fades substantially. This asymmetric structure of the flame front is attributed to the buoyancy effect. Although the buoyancy effect can impose some bias in the flame front position and the associated flame front velocity (defined later), the qualitative trends of the effects of adding fine coal particles to coarse ones revealed in the experiments are still valid.

4.2. Effect of Coal Particle Size Distribution on Flame Front Distance. The flame images captured by the high-speed video were processed by MATLAB. The flame images were first

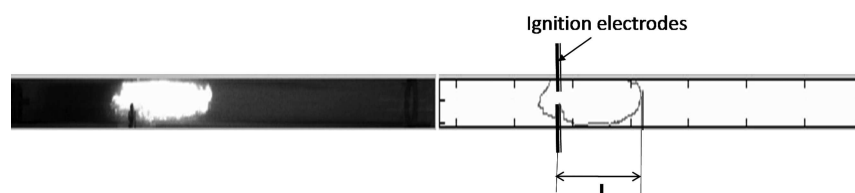


Figure 4. Extraction of flame contour and definition of flame front position.

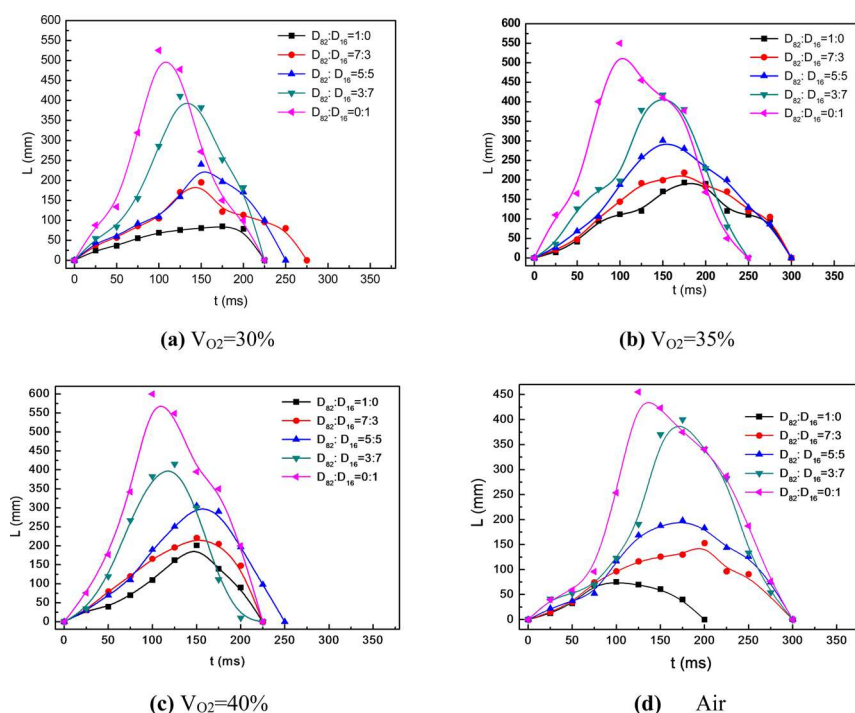


Figure 5. Variation of the flame front distance with time for the five coal samples in different atmospheres.

binarized to identify the flame envelop. Flame edge was obtained using Canny edge detector.²² An example is provided in Figure 4. The left-hand side of Figure 4 is a binarized flame image and the right-hand side shows the corresponding flame contour. The flame front position, L , is defined as the distance from the flame leading edge to the ignition electrodes.²³ It should be pointed out that there is no ambiguity in the flame front position defined in this way in the first two stages (ignition and rapid burning), but ambiguity occurs in the postflame stage when isolated burning char particles appear. In this study, the flame front position in the third stage, postflame, is identified by the leading edge of the main flame contour, excluding the isolated small pockets ahead of the main contour.

Figure 5 displays the evolution of the flame front position during flame propagation for different coal particle size distributions, i.e., for different mixing proportions of D_{82} and D_{16} in the coal samples, and for combustion in three different O_2/CO_2 atmospheres and in air. It is evident from Figure 5 that the coal sample consisting of only D_{82} has the shortest distance, while the coal sample of pure D_{16} reaches the maximum distance, regardless of the atmosphere. In addition, the maximum distance reached by a coal flame becomes longer with increasing mixing ratio of D_{16} in the coal sample.

When the oxygen mole fraction is 30% in the O_2/CO_2 atmosphere, Figure 5a, the distance of D_{82} coal flame grows very slowly and reaches a maximum value of only 84.8 mm at 175 ms. It can be seen from Figure 5d that the combustion of

D_{82} in air reaches a similar maximum flame distance of about 80 mm; however, the flame front distance of D_{82} in air grows faster and reaches its maximum distance earlier at about 100 ms than in the O_2/CO_2 atmosphere of 30% O_2 , Figure 5a. A plausible explanation for this difference lies in the higher specific heat of CO_2 than N_2 , and the diffusion rate of O_2 in N_2 is higher than in CO_2 , i.e., the higher specific heat of CO_2 in the O_2/CO_2 atmosphere at 30% O_2 concentration effectively retards the temperature rise of the gas phase, which in turn slows down the flame propagation. On the other hand, the distance of the D_{16} flame front increases rapidly after ignition and reaches 88.1 mm at 25 ms, exceeding the maximum distance of the D_{82} flame front, Figure 5a. Afterward, the D_{16} flame continues to propagate rapidly to reach a maximum distance of 525.2 mm at 100 ms, Figure 5a. Mixing a moderate amount of D_{16} into D_{82} according to $D_{82}:D_{16} = 7:3$ enhances the early flame development and improves the flame propagation velocity. This coal flame front distance reaches its maximum value of 195 mm at 150 ms in the O_2/CO_2 atmosphere of 30% O_2 concentration, Figure 5a. As the proportion of D_{16} in the coal sample is further increased, the ignition and flame propagation characteristics are further improved, i.e., the maximum coal flame front distance reaches a larger value at a shorter time after ignition, Figure 5a. The coal flame front distance reaches its maximum length of 240.1 mm at 150 ms for $D_{82}:D_{16} = 5:5$ and 410.8 mm at 125 ms when $D_{82}:D_{16}$ is 3:7.

When the oxygen concentration in the O_2/CO_2 atmosphere is increased to 35%, Figure 5b, the D_{82} flame front distance becomes significantly longer compared to that at 30% oxygen concentration shown in Figure 5a. The D_{82} flame front distance reaches its maximum length of 193.4 mm at 175 ms, Figure 5b, which is a factor of 2.23 of that at 30% O_2 . At 35% O_2 concentration, the D_{16} coal flame reaches a maximum distance of more than 500 mm at 100 ms, Figure 5b. The increase in the oxygen concentration in the O_2/CO_2 atmosphere has two effects. On one hand, it leads to a higher burning intensity of volatile and higher flame temperature. On the other hand, it lowers the specific heat of the O_2/CO_2 mixture. Both effects enhance the early flame development and subsequent propagation. The increase in ratio of D_{16} in the coal sample improves the flame front distance before the maximum value at a given time after ignition as shown in Figure 5. When the oxygen concentration is 35%, for D_{82} to D_{16} mass ratios of 7:3, 5:5, and 3:7, the maximum flame front distances are 218.4 mm at 175 ms, 300.8 mm at 150 ms, and 417.8 mm at 150 ms, respectively. At an even higher oxygen concentration of 40% in the O_2/CO_2 atmosphere, Figure 5c, the flame front distance of all the five coal samples increases faster with time to reach a higher maximum value at an earlier time after ignition than those at 35% oxygen concentration.

Figure 6 shows the maximum flame front distances of the five coal samples burning in the four oxidizers (three O_2/CO_2

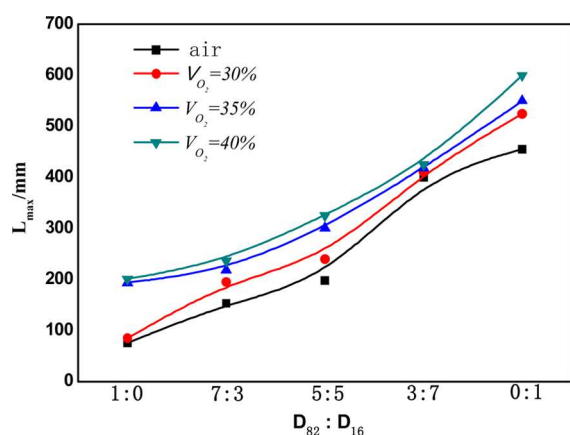


Figure 6. Maximum flame front distance of the five coal samples in different oxidizing atmospheres.

atmospheres and air). It is evident that the maximum flame front distance of D_{16} is much higher than that of D_{82} . The maximum flame front distances increase with increasing proportion of D_{16} in the coal samples, regardless of the oxidizing atmosphere. The increase in the oxygen concentration also results in a larger maximum flame front distance, especially at a higher proportion of D_{16} in the coal sample. Therefore, it can be stated that the coal ignition and flame propagation characteristics of coal particles are affected greatly by both the coal particle size distribution and the oxidizer composition. Increasing the proportion of small sized particles, i.e., D_{16} , or the oxygen concentration can enhance the coal ignition characteristics and improve the flame front distance.

4.3. Effects of Coal Particle Size Distribution on the Flame Propagation Velocity. To quantify the influence of particle size distribution on the combustion characteristics of pulverized coal, the variation of the flame front propagation velocity of the five coal samples with time was analyzed. The

flame front propagation velocity was evaluated by taking the derivative of the flame front distance with respect to time according to the distance curve.

Figure 7 displays the flame front propagation velocities of the five coal samples in the four different oxidizing atmospheres. At the early stage of flame development between 0 and about 25 ms, the flame propagation velocity displays a high sensitivity to the coal particle size distribution (characterized by the ratio of D_{82} to D_{16}) in the O_2/CO_2 atmospheres, Figures 7a–c, but not in air, Figure 7d. It can be observed from Figure 6 that there are two types of flame propagation velocity vs time variation: one is single peaked, i.e., the flame propagation velocity first increases monotonically with time to reach a peak and then decreases monotonically, and the other is double peaked or M-shaped, i.e., the flame propagation velocity first increases to reach a certain value and then decreases, at longer times it increases again to reach a second peak and finally decreases. The propagation velocity of the D_{82} (coarse coal particles) flame in the O_2/CO_2 atmosphere of 30% oxygen concentration is single-peaked and fairly slow to remain below 1 m/s, Figure 7a. For the fine coal particles D_{16} , the flame front propagation velocity displays a clear M-shaped variation with time in the atmospheres of O_2/CO_2 at 30% and 35% oxygen concentrations, Figures 7a and b, and in air, Figure 7d. However, its flame propagation velocity is essentially single-peaked in the O_2/CO_2 atmosphere at 40% oxygen concentration, Figure 7c. For the other coal samples comprising a mixture of D_{82} and D_{16} , their flame front propagation velocities are in general M-shaped in the O_2/CO_2 atmosphere of 30% O_2 concentration and in air. The M-shaped flame propagation velocity variation with time may be explained by the depletion of oxygen due to gas-phase reactions and the movement of coal particles into fresh oxidizer. For example, for fine coal particles D_{16} in the O_2/CO_2 atmosphere at 30% O_2 , these fine particles have a faster volatile release rate due to their faster temperature rise. The initial volatile release and reactions (gas-phase), which contributes to the early flame development and propagation, consume oxygen around the flame front. The decrease in the oxygen concentration within the flame zone, especially in the cases of the O_2 concentrations of 30% and 35%, slows down the reaction velocity near the end of the primary gas-phase combustion. As the particle temperature increases further, more volatile matter is released and mixed with the fresh oxidizer, the burning rates accelerate, and the flame front propagation velocity increases again. Moreover, the heat release from the combustion of volatile and char particles results in a large expansion of the gas–particle mixture that also accelerates the flame propagation. For the case with the highest O_2 concentration of 40% considered, there is likely sufficient O_2 for the burning of primary volatile matter without causing considerable deceleration of the flame front. This is likely why the flame front propagation velocity curves at 40% O_2 mole fraction show nearly single peak except the case with the coal size of whole D_{82} , Figure 7c.

The coarse coal particles (D_{82}) cannot reach similar temperatures to those of the fine particles rapidly and hence release less volatile matters upon ignition. Therefore, the flame size is small and the flame propagation velocity is slow, Figure 7b and c, or has no second peak, Figure 7a and d. When increasing the proportion of D_{16} in the coal sample, the coal particles can reach higher temperatures and there is a larger amount of volatile matter released after ignition. Consequently, the flame front propagation velocity increases. The increase in

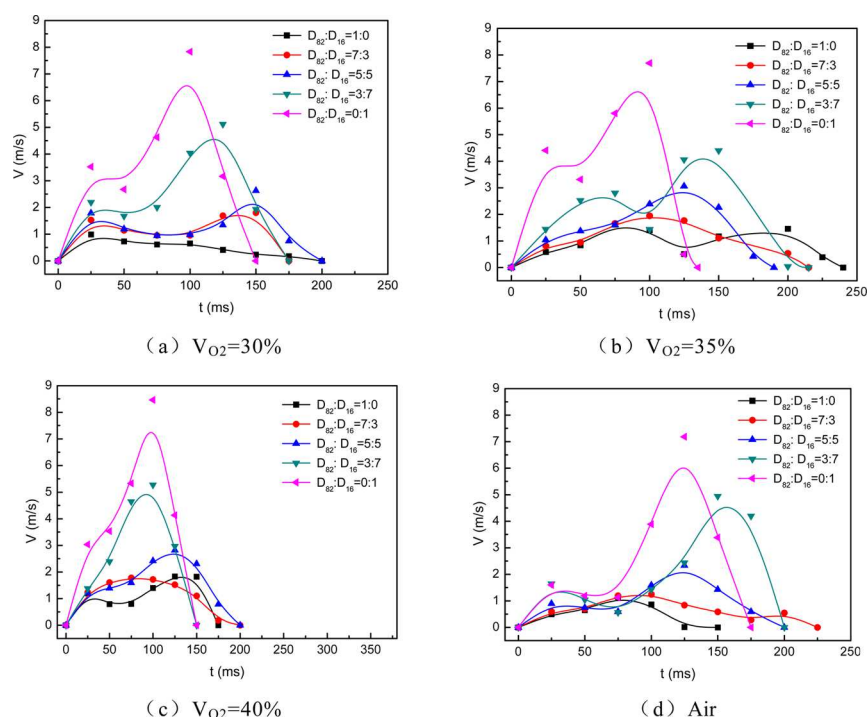


Figure 7. Variation of the flame front propagation velocity with time for the five coal samples in the four atmospheres.

O_2 mole fraction in the O_2/CO_2 atmosphere prompts the flame propagation velocity, as expected. Overall, the flame propagation velocities of the five coal samples in the O_2/CO_2 atmosphere of 30% O_2 concentration are similar to those in air, though differences exist, especially within the first 75 ms after ignition.

Figure 8 shows the peak flame front propagation velocities of five coal samples in the four oxidizing atmosphere (three $O_2/$

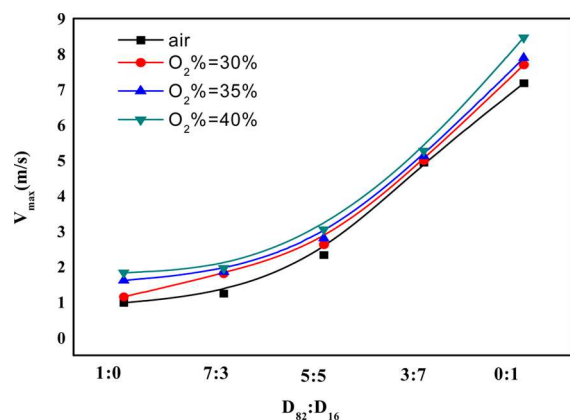


Figure 8. Maximum flame front propagation velocities of the five coal samples in the four atmospheres.

CO_2 mixtures and air). It is evident from Figure 8 that the maximum flame velocity increases significantly as more fine coal particles (D_{16}) are mixed into the coal samples. The maximum flame propagation velocity of D_{16} is about a factor of 4 to 7 of that of D_{82} , depending on the oxidizing atmosphere. In air, the maximum flame propagation velocity of D_{82} is 1.1 m/s. When the mass ratio of $D_{82}:D_{16}$ decreases to 7:3, 5:5, 3:7, the maximum flame velocity increases by a factor of 1.1, 2.1, and 4.5, respectively. In the O_2/CO_2 atmosphere of 30% O_2

concentration, the maximum flame propagation velocity of D_{82} is 1.01 m/s. With decreasing the ratio of $D_{82}:D_{16}$ from 7:3, 5:5, to 3:7, the maximum flame velocity increases by a factor of 1.8, 2.7, and 5.2, respectively. At 35% O_2 concentration in the O_2/CO_2 atmosphere, the maximum flame propagation velocity of D_{82} increases to 1.6 m/s. The mixing of D_{16} into D_{82} according to the above three ratios increases the maximum flame velocity by a factor of 1.2, 1.8, and 3.1, respectively. At the highest O_2 concentration of 40% considered in the O_2/CO_2 atmosphere, the maximum flame front propagation velocity of D_{82} increases to 1.83 m/s. The addition of D_{16} to D_{82} according to the above three ratios increases the maximum flame front velocity by a factor of 1.02, 1.5, and 2.8. These results clearly indicate that the maximum flame front propagation velocity increases with increasing the O_2 concentration in the O_2/CO_2 atmosphere and with increasing the proportion of D_{16} in the coal sample.

4.4. Numerical Results of Coal Burning Process in Hot O_2/CO_2 Atmospheres. To gain a deeper understanding of the effect of mixing fine particles to the coarse ones on the heat transfer, devolatilization, and subsequent ignition processes of coal particles in a hot gas, numerical calculations were conducted using the numerical model described in section 3. The initial gas and particle temperatures are 1100 and 300 K, respectively.

The numerical model is first validated by applying it to predict the combustion of coal particles in O_2/CO_2 atmospheres experimentally investigated in ref 24. The evolution of the modeled and measured particle temperatures with time is compared in Figure 9. It is evident that the particle temperature increases with increasing the oxygen concentration and the modeled particle temperatures are in good agreement with the experimental data at all three oxygen concentrations, suggesting that the numerical model is capable of reproducing the heat transfer, devolatilization, and the subsequent ignition process of coal particles in a hot gas.

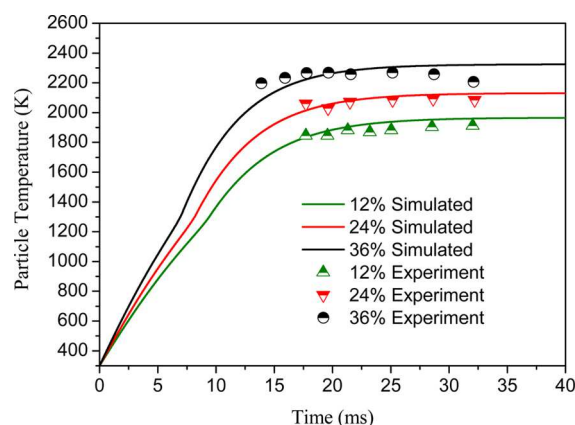


Figure 9. Comparison of the simulated particle temperatures with the experimental data²⁴ for coal particle burning in O_2/CO_2 atmospheres of different oxygen concentrations.

The modeled evolutions of normalized particle mass (by the initial value) and the temperature of the coarse particle for different coarse-to-fine coal particle mass ratios are shown in Figure 10. In the numerical simulations the five coal samples are comprised of two monodisperse particles of 16 and 82 μm . It should be emphasized that in Figure 10, the particle mass and temperature variations with time are for the coarse particles of 82 μm , except for the case of $D_{82}:D_{16} = 0:1$, in which the results are for the fine particles of 16 μm . The temperature of fine particles rises very rapidly and the devolatilization of these fine particles starts almost immediately after they are exposed to the hot environment and finishes at 2 ms, Figure 10a. On the other hand, the temperature rise of the coarse coal particles is much slower. Correspondingly, the devolatilization of these coarse particles only starts at about 8 ms and completes at about 16.5 ms, Figure 10a. It is seen from Figure 10 that mixing fine particles to the coarse ones has a significant influence on the evolution of particle mass and temperature of the coarse particles. Specifically, as more fine particles are mixed to the coarse ones, the particle temperature rise is much faster, Figure 10b, and the particle mass starts to decrease earlier and at a higher rate, Figure 10a. The ignition and subsequent flame propagation processes of coal particles are significantly influenced by the devolatilization rate, which in turn is strongly dependent on the particle temperature rise rate. The results shown in Figure 10 clearly indicate that the particle temperature rise, devolatilization, and ignition are significantly enhanced by mixing more fine coal particles. Although the

flame propagation process is not modeled, it can also be stated based on results shown in Figure 10 that mixing more fine coal particles to the coarse ones also accelerates the flame propagation speed, which is observed experimentally as discussed earlier. The fundamental reason that superfine samples are beneficial to the coal ignition lies in the much larger specific surface areas (surface area-to-volume ratio) of fine coal particles, leading to much faster temperature rise when they are exposed to an energy source, such as a hot gas stream or an ignitor.

Figure 11 displays the devolatilization times of the five coal samples in the four oxidation atmospheres. The devolatilization

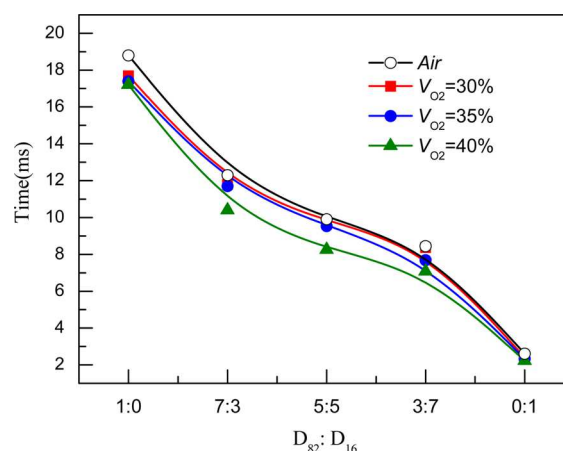


Figure 11. Devolatilization times of the five coal samples in the four oxidation atmospheres.

time is obtained from the particle mass change curve with the time shown in Figure 10a when the M_p/M_{p0} decreases to $1 - V$, i.e., when all the volatile content is released. It can be seen that the devolatilization times of the coarse particles, i.e., $D_{82}:D_{16} = 1:0$, are about eight times those of the fine particles ($D_{82}:D_{16} = 0:1$) in all the four oxidation atmospheres. As more fine coal particles are mixed into the coarse ones, the devolatilization time is significantly reduced. In the coal sample with $D_{82}:D_{16} = 7:3$, i.e., there are 30% fine coal particles on mass basis in the coal sample, the devolatilization times are shortened by about 1/3 (from about 18 ms to about 12 ms), compared to those of the pure coarse particles. At 50% mixing ratio, i.e., $D_{82}:D_{16} = 5:5$, the devolatilization times are reduced by almost half (from about 18 ms to about 9 ms). When the fine particles reach 70% of the coal sample, the devolatilization times are further

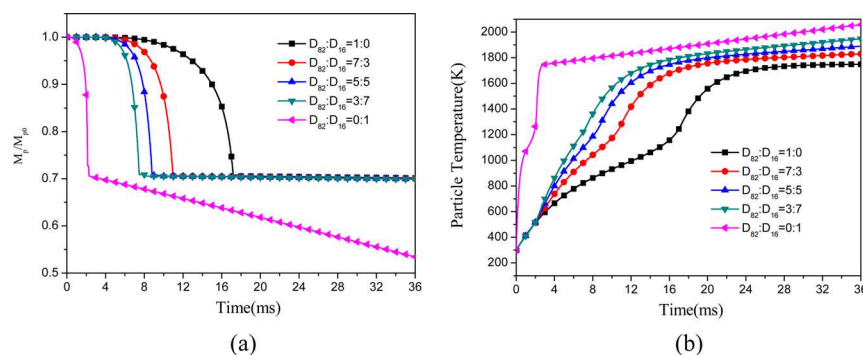


Figure 10. Evolutions of the normalized particle mass and coarse particle temperature of the five coal samples in an O_2/CO_2 atmosphere at oxygen concentration of 35% (line for $D_{82}:D_{16} = 0:1$ is for the fine particles).

reduced. The oxygen concentration also affects the devolatilization process. A higher oxygen concentration results in a shorter devolatilization time for a given coal sample. The oxygen concentration seems to have a larger effect on the devolatilization process in the presence of coarse particles in the coal sample, where the increase in oxygen concentration from 30 to 40% leads to about 1.5 ms reduction in the devolatilization times. The implications of the numerical results shown in Figures 10 and 11 are that the ignition and subsequent flame propagation of coal particles are more significantly enhanced as more fine coal particles are added to the coal sample. These numerical results help understand and interpret the experimental results presented and discussed above.

5. CONCLUSIONS

The effects of particle size and oxygen concentration in an O_2/CO_2 atmosphere on the initial flame development and subsequent propagation of pulverized coal in a quartz tube were investigated experimentally by using a high-speed video camera and image analysis to extract the flame front propagation and its velocity. Five coal samples formed by mixing fine coal particles with diameters less than $20\ \mu m$ and coarse coal particles with diameters between 70 and $100\ \mu m$ and four oxidizing atmospheres (three O_2/CO_2 mixtures and air) were considered in the experiments. A simplified numerical model was employed to help gain better understanding of the effects of mixing fine particles to coarse ones on the ignition of coal particles. The following conclusions can be drawn based on the present experimental results:

- (1) The coal particle size distribution characterized by the mass ratio of the coarse to fine particles has a strong impact on the flame propagation velocity and flamefront distance. Smaller coal particles lead to a shorter ignition delay and a longer flame front distance. Mixing fine coal particles with coarse ones is effective to improve the combustion performance of coal particles, such as a reduced ignition delay and an enlarged reaction zone and flame length.
- (2) The particle size distribution significantly affects the flame propagation velocity of a pulverized coal flame. The variation of the instantaneous flame propagation velocity with time is in general M-shaped or double-peaked. The flame propagation velocity of the coarsest coal particles considered in this study at 30% oxygen concentration in O_2/CO_2 atmosphere is single-peaked. For the coal sample of the finest particles considered, its flame front propagation velocity is also single-peaked when burning in the O_2/CO_2 atmosphere of 40% oxygen mole fraction. The flame of fine coal particles appears brighter, smother, and moves much faster. Mixing of fine coal particles with coarse ones is effective to improve the ignition and propagation properties of pulverized coal flames.
- (3) Numerical results indicate that mixing of fine coal particles to coarse ones leads to much faster coarse particle temperature rise and earlier devolatilization and are consistent with the experimental observations.
- (4) Increase in the oxygen concentration in an O_2/CO_2 atmosphere is beneficial to improve the ignition and flame propagation characteristics of pulverized coal flames. A higher oxygen concentration results in a longer

and faster flame. The oxygen concentration effect is stronger with increased proportion of fine coal particles in the coal sample.

The findings of this study indicate that mixing fine coal particles with coarse ones is effective in improving the ignition and flame propagation characteristics of coal combustion in O_2/CO_2 atmospheres. Further studies are required to investigate how mixing fine and coarse coal particles affects NO_x formation.

AUTHOR INFORMATION

Corresponding Authors

*Tel.: +86-555-2311816. E-mail: mingyan_gu@qq.com (M.G.).

*E-mail: hqchust@163.com (H.C.).

ORCID

Huaqiang Chu: [0000-0001-7399-5887](https://orcid.org/0000-0001-7399-5887)

Notes

The authors declare no competing financial interest.

ACKNOWLEDGMENTS

The authors gratefully acknowledge the support of the National Science Foundation of China (51376008, 51676002).

REFERENCES

- (1) Zhou, Y.; Jin, X.; Jin, Q. *Combust. Flame* **2016**, *167*, 52–59.
- (2) Yoshiie, R.; Hikosaka, N.; Nunome, Y.; et al. *Fuel Process. Technol.* **2015**, *136*, 106–111.
- (3) Yuan, Y.; Li, S.; Li, G.; Wu, N.; Yao, Q. *Combust. Flame* **2014**, *161* (9), 2458–2468.
- (4) Taniguchi, M.; Shibata, T.; Kobayashi, H. *Proc. Combust. Inst.* **2011**, *33* (2), 3391–3398.
- (5) Yi, B.; Zhang, L.; Fang, H.; Luo, Z.; Zheng, C. J. *Combust. Sci. Technol.* **2013**, *19* (3), 248–253.
- (6) Ju, W. J.; Dobashi, R.; Hirano, T. *J. Loss Prev. Process Ind.* **1998**, *11* (3), 177–185.
- (7) Chen, L.; Yong, S. Z.; Ghoniem, A. F. *Prog. Energy Combust. Sci.* **2012**, *38*, 156–214.
- (8) Rathnam, R.; Elliott, L.; Wall, T.; Liu, Y.; Moghtaderi, B. *Fuel Process. Technol.* **2009**, *90*, 797–802.
- (9) Smart, J.; Lu, G.; Yan, Y.; Riley, G. *Combust. Flame* **2010**, *157* (6), 1132–1139.
- (10) Suda, T.; Masuko, K.; Sato, J. i.; Yamamoto, A.; Okazaki, K. *Fuel* **2007**, *86* (12–13), 2008–2015.
- (11) Liu, Y.; Geier, M.; Molina, A.; Shaddix, C. R. *Int. J. Greenhouse Gas Control* **2011**, *5*, S36–S46.
- (12) Hu, Y.; Naito, S.; Kobayashi, N.; Hasatani, M. *Fuel* **2000**, *79*, 1925–1932.
- (13) Bejarano, P. A.; Levendis, Y. A. *Combust. Flame* **2008**, *153* (1–2), 270–287.
- (14) Abbas, T.; Costen, P.; Lockwood, F. C.; Romo-Millares, C. A. *Combust. Flame* **1993**, *93* (3), 316–326.
- (15) Huang, X.; Jiang, X.; Han, X.; Wang, H. *Energy Fuels* **2008**, *22* (6), 3756–3762.
- (16) Liu, J.; Jiang, X.; Shen, J.; Zhang, H. *Energy Fuels* **2014**, *28*, 5497–5504.
- (17) Gu, M.; Wu, C.; Zhang, Y.; Chu, H. J. *CO₂ Utiliz.* **2014**, *7*, 6–10.
- (18) Goshayeshi, B.; Sutherland, J. *Combust. Flame* **2014**, *161* (1–2), 1900–1910.
- (19) Kobayashi, H.; Howard, J. B.; Sarofim, A. F. *Symp. Combust., [Proc.]* **1977**, *16*, 411–425.
- (20) Zhang, J.; Pratiomo, W.; Zhang, L.; Zhang, Z. *Energy Fuels* **2013**, *27* (8), 4258–4269.
- (21) Mon, E.; Amundson, N. R. *Ind. Eng. Chem. Fundam.* **1978**, *17*, 313–321.

- (22) Canny, J. *IEEE Trans. Pattern Anal. Mach. Intell.* **1986**, 8 (6), 679–698.
- (23) Xiao, H. H.; Houim, R. W.; Oran, E. S. *Combust. Flame* **2015**, 162, 4084–4101.
- (24) Shaddix, C. R.; Molina, M. *Proc. Combust. Inst.* **2009**, 32, 2091–2098.